J Nanopart Res (2014) 16:2401
DOI 10.1007/s11051-014-2401-7

RESEARCH PAPER

# Hazard assessment of W and Mo sulphide nanomaterials for automotive use

**Ingrid Corazzari · Fabio A. Deorsola · Giulia Gulino · Elisabetta Aldieri · Samir Bensaid · Francesco Turci · Debora Fino**

Received: 11 February 2014 / Accepted: 2 April 2014 / Published online: 23 April 2014


**Abstract** Engineered nanomaterials (ENMs) are growing in interest and use due to the enhancements envisaged in many applications. ENM hazard identification and exposure scenarios are growing in interest too. Inhalation, ingestion and assimilation through skin during ENM production or use have to be considered as possible events, and potential ENM toxicity has to be investigated before new ENM-based products are placed on the market. To design new ENM-based additive in lubricants for automotive application, the European FP7 Project AddNano is investigating the use of fullerene-like inorganic nanomaterials, including transition metal disulphides. In this work, the potential toxicities of well-characterized pristine $MoS_2$ and $WS_2$ ENMs were evaluated by in vitro cellular and a cell-free chemical tests. Cytotoxicity and oxidative stress on human pulmonary epithelial cells (A549), ENM surface reactivity (free radical production and lipid peroxidation), and ENM durability in simulated biological fluids were evaluated. In all tests, $WS_2$ did not elicit a response significantly different from the negative control. $MoS_2$ showed a moderate cellular toxicity at the highest dose and was inert in all other circumstances. Both $WS_2$ and $MoS_2$ were soluble in simulated biological fluids, suggesting a short durability in vivo. The low overall biological and chemical reactivity of $WS_2$ and $MoS_2$ suggests that tested nanomaterials are unlikely to be an hazard, as far as human respiratory system is concerned. Data could be usefully implemented in the context of environmental risk assessment and life cycle assessment.

**Keywords** Fullerene-like inorganic nanomaterials · Nano-hazard assessment · Cytotoxicity · ROS · Simulated biological fluids · Environmental and health effects

I. Corazzari · G. Gulino · E. Aldieri · F. Turci (✉)
'G. Scansetti' Interdepartmental Center for Studied on Asbestos and Other Toxic Particulates, Via P. Giuria, 9, 10125 Turin, Italy
e-mail: francesco.turci@unito.it

I. Corazzari · F. Turci
Department of Chemistry, Università di Torino, Via P. Giuria, 7, 10125 Turin, Italy

F. A. Deorsola · S. Bensaid · D. Fino (✉)
Department of Applied Science and Technology, Politecnico di Torino, Corso Duca degli Abruzzi 24, 10129 Turin, Italy
e-mail: debora.fino@polito.it

G. Gulino · E. Aldieri
Department of Oncology, Università di Torino, Regione Gonzole, 10, 10043 Orbassano, TO, Italy

## Introduction

The progress associated to the manipulation of materials on a near-atomic size scale (1–100 nm) to impart new properties rises a general concern about the consequent exposure of the workers and general

population to engineered nanomaterials (ENMs) (Nel et al. 2006; Stern and McNeil 2008). In parallel, it has been clarified that the nano-sized fraction of the environmental particulate matter posesses the highest risk in pulmonary and cardiovascular diseases (Oberdorster et al. 2005). ENMs can be inhaled ingested and internalized through the skin, either unintentionally (from the environment or during industrial manufacturing) or following their desired use as diagnostic and therapeutic tools. The promising perspectives of nanotechnology challenge researchers and environmental agencies to define hazard and exposure scenarios that take into consideration the unique physico-chemical properties of ENMs (Cohen et al. 2013; Som et al. 2013; Wang et al. 2013; Xia et al. 2013). The physico-chemical features of ENMs relevant to toxicity have been examined in various recent articles and reviews (Oberdorster 2010; Zhang et al. 2012; Fubini et al. 2011; Podila and Brown 2013), but reliable and reproducible screening approaches are still needed to test the basic materials (Nel et al. 2013). Some bulk and surface physico-chemical characteristics, such as particle shape, free radical generation or quenching, hydrophilicity and solubility which in turn determines the persistence in the body compartments (i.e., bio-durability), were proven to be important in defining the toxic outcomes of ENMs (Bouwmeester et al. 2011; Donaldson et al. 2011; Fubini et al. 2010). Assessing the risks of nanomaterials use is of high priority given their expected distribution for industrial applications and the likelihood of exposure for both humans and ecosystems, directly or through release into the environment.

The use of innovative engineered ENMs incorporated into lubricants for automotive applications can lead to significant performance breakthroughs, in terms of reduction of the friction coefficient and improvement of the protection against wear. The actual anti-wear additives, based on zinc dialkyl dithiophosphates (ZDDPs), have been developed about 70 years ago (Spikes 2004), and a technological progress is expected. The most suitable candidates for ZDDPs substitution are the transition metal dichalcogenides, with the generic formula $MX_2$ (M = W, Mo; X = S, Se). These materials, mainly nanometric sulphides, can bring to substantial energy saving, reduction of the equipment maintenance and lengthening of the machine lifetime. Particularly, the use of ENMs with increased mechanical and technological qualities foreshadows the enhancement of the rheological and heat-resistance properties of lubricant oils. Furthermore, in automotive engines, sulphur and phosphorous contained into ZDDPs tend to poison catalysts for the exhaust-treatments. Increased thermal stability of $MX_2$-based ENMs could also enhance lifetime and performance of the catalysts, hence decreasing emissions.

Every project involving the mid- or large-scale production of new ENMs should face the urgency to provide an adequate assessment of the risk, not only to prevent the onset of detrimental health effects on workers and/or exposed population, but also to prevent unjustified fears which could hinder the commercialization and the acceptance of otherwise useful ENMs. The hazard evaluation of two metal-sulphide inorganic fullerene-like ENMs, namely $MoS_2$ and $WS_2$, recently synthesised (Fino et al. 2011; Deorsola et al. 2012) and employed in the context of a large multidisciplinary project on lubricant addictives for automotive usage (FP7 AddNano), was carried out.

Three main exposure scenarios were proposed during the LCA analysis (Deorsola et al. 2012; Raimondi et al. 2012), and a simplified hazard-oriented life cycle analysis was drawn (Scheme 1). The scheme highlights the dramatic variability imparted to ENM surface during its life cycle. Naked, unaltered and pristine ENM occurring in the first scenario may be toxicologically very different from the engine-exhausted fumes which may contain post-burned ENMs in the second scenario. During the recycling/disposal phase, the ENMs may further be modified by the recycling treatments and their toxicological properties largely altered. The hazard assessment currently proposed is addressed only to the potential exposure scenario 1, where the ENMs are unaltered, and consequently analyzed as prepared.

This work is aimed at the assessment of the hazard posed by $MoS_2$ and $WS_2$ ENMs in their pristine state. A set of complementary, inexpensive and easy-to-perform chemical and biochemical tests has been performed. The pristine $MoS_2$ and $WS_2$ were thoroughly characterized, and their potential toxicity was evaluated by means of cellular and cell-free tests, using human pulmonary epithelial cells (A549) and cell-free radical and oxidative reactivity, respectively. Solubility of sulphide ENMs in fluid-simulating specific cellular environments was also performed, and the biodurability of the two ENMs estimated. The modular,

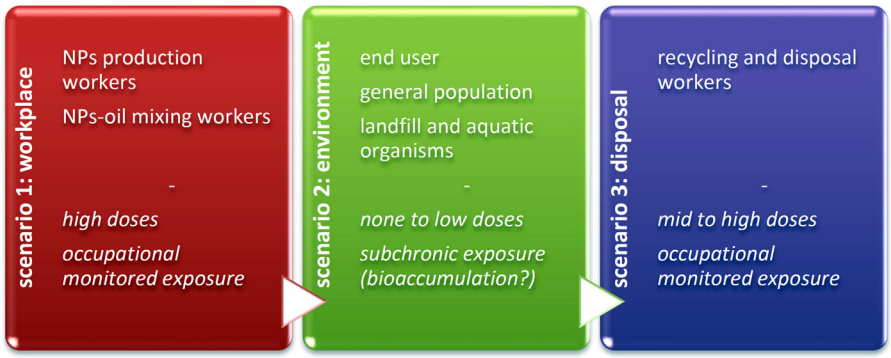


**Scheme 1** Hazard-oriented life cycle scenarios of the ENMs investigated. In the first scenario, the workplace, the workers of the manufacturing sectors are potentially exposed to naked, unaltered ENMs delivered at high doses for a short amount of time (accident). The scenario 2, the environment, illustrates the exposure scenario and the dose likely occurring during the usage of the ENMs-enhanced oil. The scenario 3 illustrates the last part of the life-cycle of the ENMs, which occurs again in an occupational setting but the workers could now be exposed to ENMs largely modified by the automotive usage

integrated approach to sort out which ENMs are unfit for the market and have to be cut-off from scale-up production is proposed as screening tool for environmental risk assessment (ERA) and life cycle assessment (LCA).

## Materials and methods

### Reagents

When not otherwise specified, all the reagents were from Sigma Chemicals (Sigma-Aldrich S.r.l. Milan, Italy), and all the solutions employed were prepared with Milli-Q ultrapure water system (Millipore S.p.A., Vimodrone, Milan).

### ENMs synthesis and physico-chemical characterization

$WS_2$ fullerene-like spherical ENM was produced by NanoMaterials Ltd. through a reaction between $WO_3$ and $H_2S$, in reducing atmosphere at high temperatures. Amorphous $MoS_2$ ENM was obtained by Politecnico di Torino, Department of Applied Science and Technology, through a wet synthesis technique that involved a simple and scalable process as well as low-cost reactants (Deorsola et al. 2012). Both ENMs were developed and synthesised within the framework of the EU FP7 project AddNano by NanoMaterials Ltd. and Politecnico di Torino, Department of Applied Science and Technology, respectively.

$WS_2$ was developed at Weizmann Institute by Tenne and coworkers (Margulis et al. 1993; Tenne et al. 1992) and subsequently commercialized by NanoMaterials Ltd. The synthesis is based on the reaction in a fluidized bed of the metal oxide particles with $H_2S$ in a reducing atmosphere at high temperature. At the beginning of the process, one or two monomolecular layers of $WS_2$ are formed by means of the reaction between the tungsten oxide and the $H_2S$ gas. In the meanwhile, hydrogen diffusion completely reduces the oxide core to $W_{18}O_{49}$, and the oxide core is converted to tungsten disulphide by a slow diffusion-controlled reaction with $H_2S$ (Feldman et al. 1996). The control of the process parameters has allowed to strictly design the size, shape and distance of layers in the onion-like structure.

$MoS_2$ was obtained by means of a wet chemical synthesis in an aqueous solution employing ammonium molybdate, citric acid and ammonium sulphide as starting materials. The process is based on the preparation of an aqueous solution containing citric acid and ammonium molybdate in suitable amounts. In the solution, a complex between molybdenum (IV) and citrate is formed, and this reacts with a suitable content of ammonium sulphide in order to precipitate $MoS_2$ ENM. This synthesis route is extremely versatile and easily scalable: a continuous micro-mixer is currently being used for ENM precipitation with a strict control of the particle diameter (Santillo et al. 2012; Bensaid et al. 2014).

The pristine $MoS_2$ and $WS_2$ were thoroughly characterized by studying microstructure and morphology

(FESEM and TEM), particle size distribution (DLS), surface charge in aqueous suspension (electrophoretic mobility, ELS) and surface area (BET).

*Electron microscopy*

The samples for FESEM observations (Leo Supra 40) were prepared by suspending some products in isopropanol, thorough ultrasonic mixing for half an hour, and subsequently by placing a drop of the dispersion on a copper grid coated with a layer of amorphous carbon.

Specimens for TEM studies were prepared by slow evaporation of a drop of highly diluted fullerene dispersion in ethanol after deposition onto a discontinuous carbon film mounted on a copper grid. The TEM observations were performed on a JEOL 2010 FEG microscope operating at 200 kV accelerating voltage equipped with an ISIS EDS spectrometer (probe size of 5 nm).

*Particle size distribution*

The size of aggregates was measured by Dynamic Light Scattering (DLS) (Zetasizer Nano-ZS, Malvern Instruments, Worcestershire, UK, detection limits 1 nm–6 μm). This technique measures a hydrodynamic size correlated to the measurement of dynamic fluctuations of light-scattering intensity caused by Brownian motion of the particles during movement in ultrapure water. The ENMs were suspended in water and sonicated for 2 min with a probe sonicator to achieve optimal sample dispersion (Sonoplus, Bandelin, Berlin, Germany).

*Specific surface area (BET)*

Surface area of the sulphide ENMs was measured by means of the well-known BET method based on $N_2$ adsorption at 77 K (ASAP 2020 Micrometrics, Norcross, GA).

*Surface charge/ζ-potential*

The ζ-potential was evaluated by means of Electrophoretic Light Scattering (ELS, Zetasizer Nano-ZS, Malvern Instruments, Worcestershire, U.K) on the dusts previously suspended in cell growth culture medium (Dulbecco's Modified Eagle Medium, DMEM, pH 7.4, Sigma-Aldrich) and sonicated for 2 min with a probe sonicator (4 W/ml, ca. 20 kHz, Sonoplus, Bandelin, Berlin, Germany).

*X-ray florescence spectroscopy (micro-XRF)*

All samples were analyzed by means of a RIGAKU ZSX100E equipped with a Rh X-ray tube and TAP, PET, LiF1, Ge, RX61 and RX45 analysis crystals. Samples were prepared by pressing ENMs into thin discs with a diameter of 20 mm and a thickness of 2 mm. The samples were analyzed in at least 20 different points.

Cellular test

$WS_2$ and $MoS_2$ potential toxicity was evaluated by means of cellular tests, using human pulmonary epithelial cells (A549), a robust model for lung exposure to and oxidative reactivity of (nano) particulate. Cytotoxicity was evaluated measuring the LDH released in the extracellular space, and the ENM-induced oxidative stress was quantified by measuring nitric oxide (NO) production and glutathione (GSH) depletion. Human pulmonary epithelial cells (A549), provided by Istituto Zooprofilattico Sperimentale 'Bruno Ubertini' (Brescia, Italy), were cultured in 60-mmdiameter Petri dishes in culture medium RPMI-1640 (Gibco, Paisley, UK) supplemented with foetal bovine serum (FBS) 10 % and penicillin/streptomycin 1 % up to confluence. Plasticware for cell culture was from Falcon (Becton–Dickinson, Franklin Lakes, NJ). The ENMs were used at the following concentrations: 10, 25 and 50 $\mu g/cm^2$. To allow a better diffusion in the medium, the samples were sonicated 90 s before incubation with cells. Cells were incubated for 24 h in the absence or presence of different concentration of particles. After 24 h, the supernatants were collected and centrifuged at $13{,}000 \times g$ for 90 min; the cell monolayers were washed twice with PBS (Phosphate-Buffered Saline, pH 7.4), then detached, resuspended in PBS and sonicated on ice with a 10 s burst. The protein content of cell monolayers and cell lysates was assessed with the BCA kit.

Cytotoxicity

Cells were washed with fresh medium, detached with trypsin/EDTA (0.05/0.02 % v/v), washed with PBS,

suspended in 0.8 ml of TRAP (82.3 mM triethanolamine, pH 7.6) and sonicated on ice with a 10 s burst. Aliquots of cell lysate and of extracellular medium were diluted with TRAP and supplemented with 0.5 mM sodium pyruvate and 0.25 mM NADH to start the reaction. The reaction was followed for 10 min, measuring the loss of absorbance at 340 nm (37 °C) with a Synergy HT microplate reader (Bio-Tek Instruments, Winooski, VT). Both intra and extracellular enzymatic activity is indicated as µmol NADH oxidized/min/dish, then extracellular LDH activity (LDH out) was calculated as percentage of the total (intracellular + extracellular) LDH activity (LDH tot) in the dish.

### NO production

To evaluate whether the ENMs are able to induce an inflammatory response, nitrite production and accumulation in the extracellular medium was detected. Nitrite is the stable oxidation product of NO, and its production has been evaluated through the Griess method (Ghigo et al. 1998). NO is a fundamental molecule in the inflammatory process, because of its great reactivity with superoxide anion and the subsequent production of peroxynitrite, one of the main responsible for lipid peroxidation and DNA damage. Nitrite concentration was expressed as nmol nitrite/mg cell protein.

### Glutathione consumption

GSH and GSSG were measured as previously described (Vandeputte et al. 1994), using a modified glutathione reductase-DTNB recycling assay. Cells were washed with PBS and 600 µl 0.01 N HCl were added to each cell monolayer. After gentle scraping, the cells were sonicated 10 s, and the proteins were precipitated by adding 120 µl of 6.5 % 5-sulfosalicylic acid to 480 µl of lysate. Each sample was placed in ice for 45 min and then centrifuged for 15 min at 13,000×*g* (4 °C). The total glutathione was measured in 20 µl of the cell lysate with the following reaction mix: 20 µl stock buffer (143 mM $NaH_2PO_4$, 63 mM EDTA, pH 7.4), 200 µl daily reagent [10 mM 5,5′-dithiobis-2-nitrobenzoic acid (DTNB), 2 mM NADPH in stock buffer], and 40 µl glutathione reductase (8.5 U/ml). The content of GSSG was obtained after derivatization of GSH with 2-vinylpyridine (2VP): 10 µl of 2VP were added to 200 µl of cell lysate, and the mixture was shaken at room temperature for 90 min. Glutathione was then measured in 40 µl of sample as described. The kinetics of reaction was followed at 415 nm for 10 min (to check response linearity) using a Synergy HT microplate reader. Results were expressed as nmol of glutathione/mg cellular protein. For each sample, GSH was obtained by subtracting GSSG from total glutathione.

### Oxidative potential

The biochemically relevant reactivity of $WS_2$ and $MoS_2$ was investigated by quantifying the potency to induce peroxidation damage of unsaturated lipid (lipoperoxidation), and generate free-radical in solution. Peroxidation of linoleic acid, used as a model of cell membrane lipid, and free radical reactivity toward hydrogen peroxide and formate ion, two target molecules largely employed to measure ROS production from inorganic particulate in cell-free tests, have been followed by means of colorimetric thiobarbituric acid assay (TBA) and spin-trapping technique (EPR spectroscopy), respectively.

#### *Lipoperoxidation*

The assay, commonly used as an index of oxidative potential (Turci et al. 2013), is based on the reactivity of MDA, a colourless end-product of degradation, with tiobarbituric acid (TBA) to produce a pink adduct that absorbs at 535 nm. 9 mg of the dusts were suspended in 3 ml of a buffered (sodium phosphate buffer 10 mM, pH 7.4) micellar dispersion of linoleic acid (1 mM) containing the 2.5 % w/w of ethanol. The mixture was stirred in the dark at 37 °C for 72 h. The lipid peroxidation was stopped by adding 0.1 ml of an ethanolic solution of butyl hydroxyl toluene (BHT, 0.2 % w/w) to the suspension. The dust was removed by centrifugation (20,000 RPM, 30 min). 2 ml of a solution of TBA (0.034 M) containing HCl (0.25 M) and trichloroacetic acid (TCA, 0.92 M) were added to 1 ml of the solution, and the resulting mixture was heated in a boiling water bath for 30 min to favour the formation of the pink complex. After cooling in an ice bath, 3 ml of 1-butanol were added to extract the coloured complex. The absorbance at 535 nm was measured on the organic phase by means of a UV/Vis

spectrophotometer (Uvikon, Kontron Instruments, Inc., Everett, MA). The test was also carried out (i) in the absence of dust (blank) and (ii) in the presence of $TiO_2$ (P25 Aeroxide, Evonik) at the same concentration of the samples studied (positive control). The experiments were repeated three times.

*Free radicals generation study*

The release of radical species was monitored by EPR spectrometry (Miniscope 100 X-band EPR spectrometer, Magnettech, Germany) by means of the spin-trapping technique with 5-dimethyl-1-pyrroline-*N*-oxide (DMPO, Alexis-Biochemicals, Lausen, Switzerland) employed as spin trap molecule.

*Generation of hydroxyl radicals* 8 mg of the dusts were suspended in 1.25 ml of a buffered solution (phosphate buffer 0.2 M, pH 7.4) containing DMPO (0.034 M) and $H_2O_2$ (0.080 M). After 10, 30 and 60 min of incubation under continuous stirring, the EPR spectra were recorded on the suspension. The experiments were carried out also in the absence of dust (blank solution) and in the presence of indium/tin oxide (ITO, at the same concentration of the dust samples) employed as positive control. All the experiments were repeated three times.

*Generation of carbon centred radicals* 10 mg of the dusts were suspended in 1 ml of a buffered solution (phosphate buffer 0.25 M, pH 7.4) of sodium formate (1 M) and DMPO (0.085 M). After 10, 30 and 60 min of incubation under continuous stirring, the EPR spectra were recorded on the suspension. The experiments were carried out also in the absence of dust (blank solution) and in the presence of indium/tin oxide (ITO) employed as positive control at the same concentration of the dust samples. All the experiments were repeated three times.

Ion release in simulated cellular fluids

Solubility of sulphide ENMs in fluids simulating specific cellular environments (Gamble's solution and PSF) was performed. The bio-durability was quantified by measuring the kinetics of ion release in the two simulated biological fluids with ICP–AES. The release of metal ions was studied under static leaching conditions incubating the ENMs in modified Gamble's solution (GS) and phagolysosomal simulant fluid (PSF), commonly used to simulate different interstitial conditions in the lung (Marques et al. 2011; Turci et al. 2012). The ENMs were suspended (3 mg/ml) in GS or PSF at 37 °C for 1 week and 1 month. After the incubation, the suspension was centrifuged ($20{,}000 \times g$, 30 min) and then filtered through acetate membrane filter (cut off 0.20 μm) to remove any residual particle. The amount of Mo or W in the supernatant was measured by means of ICP–AES. All the experiments were carried out three times.

*Gamble's solution*

Modified Gamble's solution was prepared according to Groppo and coworkers (2005). The chemical composition of the solution is reported in Table 1. The pH was adjusted to 7.4 by bubbling $CO_2$ in the solution.

*Phagolysosomal simulant fluid (PSF)*

Phagolysosomal simulant fluid (PSF) was prepared according to Stefaniak et al. (2005). The chemical composition of PSF (pH 4.6) is reported in Table 2.

In both GS and PSF, ultrapure MilliQ (Millipore, Billerica, MA, USA) water was used to prepare the buffer, and sodium azide (0.1 %) was added in order to prevent the growth of algae or bacteria.

**Table 1** Composition of the Gamble's solution used in this study ($CO_2$ saturated, pH 7.4)

| Component | Concentration (mg/l) |
|---|---|
| $MgCl_2 \cdot 6H_2O$ | 212 |
| NaCl | 6,415 |
| $CaCl_2 \cdot 4H_2O$ | 318 |
| $Na_2SO_4 \cdot 10H_2O$ | 179 |
| $Na_2HPO_4$ | 148 |
| $NaHCO_3$ | 2,703 |
| ($Na_2$ tartrate)$\cdot 2H_2O$ | 180 |
| ($Na_3$ citrate)$\cdot 2H_2O$ | 144 |
| Na lactate | 175 |
| Glycine | 118 |
| Na pyruvate | 172 |

Sodium azide (0.1 % w/w) was added to prevent the formation of algae and bacteria

**Table 2** Composition of the Phagolysosomal simulant fluid (PSF) (pH 4.6)

| Component | Concentration (mg/l) |
|---|---|
| $Na_2HPO_4$ | 142.0 |
| NaCl | 6,650.0 |
| $Na_2SO_4$ | 71.0 |
| $CaCl_2{\cdot}2H_2O$ | 29.0 |
| Glycine | 450.0 |
| K hydrogen phthalate | 4,084.6 |

Sodium azide (0.1 % w/w) was added to prevent the formation of algae and bacteria

*ICP–AES quantification of ions released*

ICP–AES analyses of Mo and W were performed with an IRIS II Advantage/1000 Radial Plasma Spectrometer by Thermo-Jarrel Ash Corp. The optical system is sealed with inert gas, with no moving parts, high resolution (ER/S) capable. The Echelle grating & Dispersion prism monochromator range extends between 165 and 800 nm, with an optical resolution of 0.007 nm (at 200 nm). The photo device is a Charge Injection Device Camera frozen to −50 °C.

Statistical analysis

All data in text and figures are provided as mean ± SEM. The results were analyzed by a one-way Analysis of Variance (ANOVA) and Tukey's test. $p < 0.05$ was considered significant.

## Results and discussion

Physico-chemical characterization of the ENMs

*Microstructural characterization (FESEM and TEM)*

The FESEM characterization of the $MoS_2$ and $WS_2$ ENMs is reported in Fig. 1. Both ENMs showed a similar morphology. On one hand, the dimension of the $MoS_2$ agglomerates was higher than that of the $WS_2$ ones (see Fig. 1a, c), whereas $MoS_2$ primary particles looked slightly smaller than the $WS_2$ ones (Fig. 1b, d). Nevertheless, in both cases the dimension of primary particles was less than 50 nm.

TEM observations, reported in Fig. 2, allow to appreciate the dimension of the ENMs, in both cases

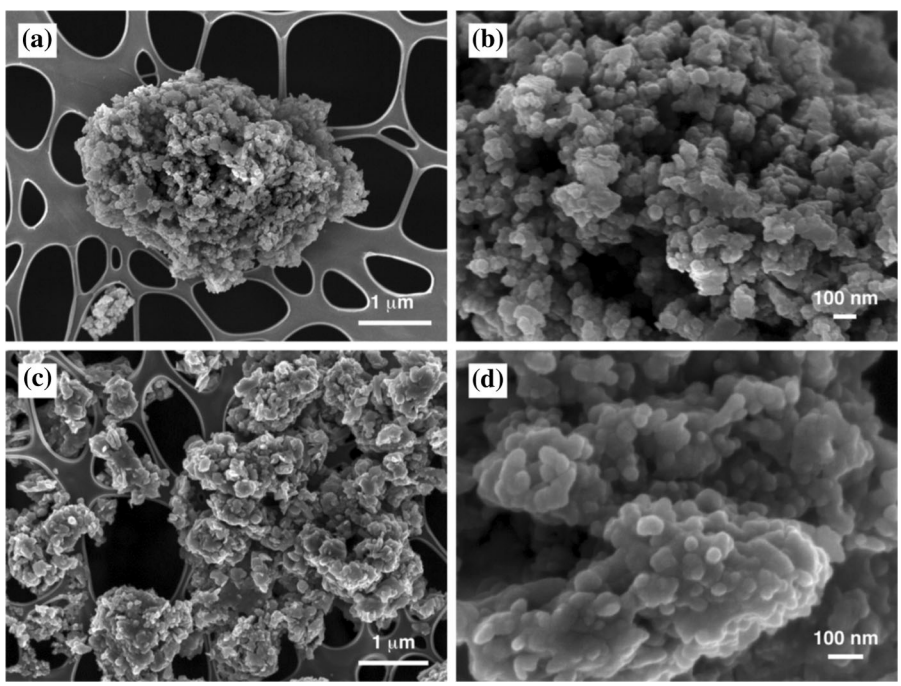


**Fig. 1** FESEM micrographs of the $MoS_2$ (**a**, **b**) and $WS_2$ (**c**, **d**) ENMs employed in the hazard assessment

below 100 nm. $MoS_2$ showed a regular and uniform shape (Fig. 2a), whereas the morphology of $WS_2$ appeared less defined (Fig. 2c), even if the average diameter was smaller than molybdenum sulphide. This trend was confirmed by the images at higher magnification. $MoS_2$ ENM showed the outer shell (about 10–20 nm) constituted of planes with the 'onion-like' structure, and the inner part looked as an hollow sphere (see Fig. 2b). On the other hand, the $WS_2$ ENM showed more irregularities in the outer layers, also constituted of planes in the 'onion-like' configuration, with in some parts a sort of beginning of exfoliation (Fig. 2d).

In Table 3, the hydrodynamic size of the particles suspended in pure water is reported as $\zeta$ average values. Both samples exhibited aggregates characterized by a wide range of diameters as evidence by the high PDI values. Both the samples exhibited similar *Z*-average values.

From a toxicological point of view, the aggregation of synthetic nanoparticle into larger sub-micrometric aggregate may remarkably impact on its potential hazard. In fact, it is widely held that inhaled nanoparticle with a diameter of few nanometres may cross the alveolar epithelium and translocate into the blood circulation or even circumvent the tight blood–brain barrier and eventually attain the brain (Oberdorster et al. 2004). However, many ENMs, including $WS_2$ and $MoS_2$, show, in vacuum, nanometric primary particle size (TEM, Fig. 2), but in aqueous media are indeed composed of larger aggregated nanoparticles that are held by strong electrostatic or covalent bonds (*Z* average diameter, Table 3). The observed aggregation makes the massive diffusion of these kind of

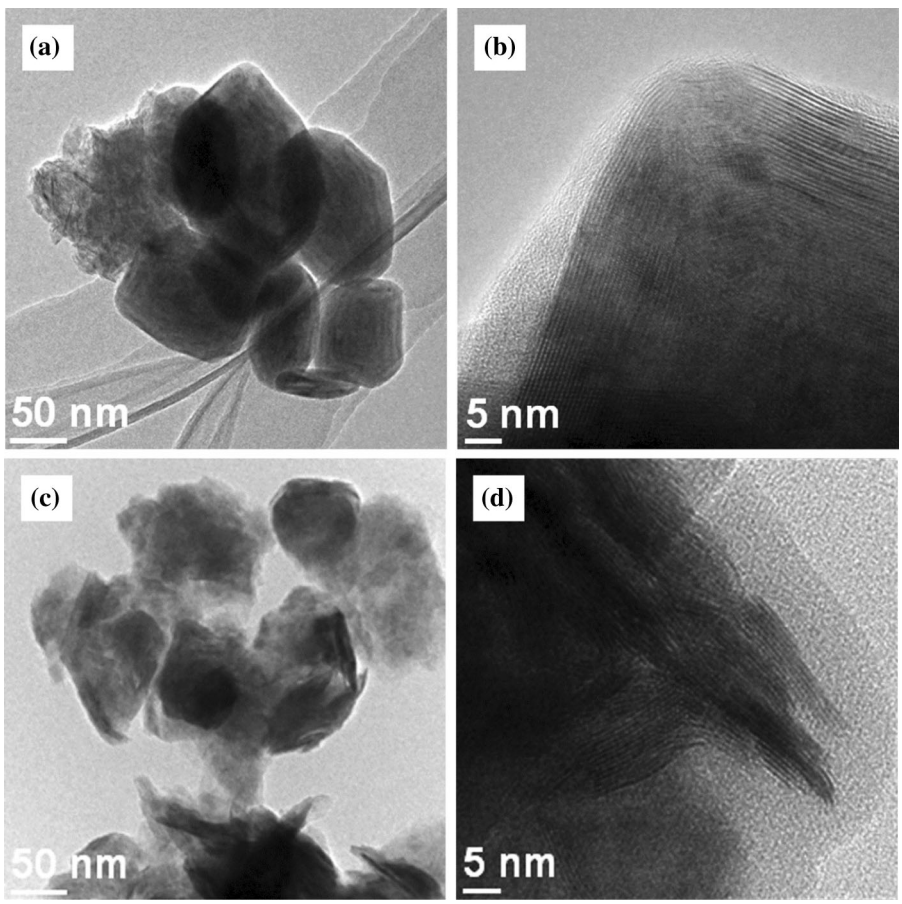


**Fig. 2** TEM micrographs of the $MoS_2$ (**a**, **b**) and $WS_2$ (**c**, **d**) ENMs employed in the hazard assessment

**Table 3** Summary of the main physico-chemical properties relevant for the interaction of inorganic ENMs with cells and tissues

| | Z average diameter ± SD (nm) | CONTIN peak ± SD (nm) | PDI ± SD | ζ potential ± SD (mV) @ pH 7.4 in cell growth culture medium | BET surface area ($m^2$/g) | Me/S molar ratio (XRF–EDS) |
|---|---|---|---|---|---|---|
| $WS_2$ | 390 ± 5 | 461 ± 45 | 0.35 ± 0.03 | −11 ± 1 | 27.4 | 1:2 |
| $MoS_2$ | 361 ± 6 | 451 ± 24 | 0.24 ± 0.01 | −10 ± 1 | 9.2 | 1:2.1 |

Hydrodynamic size (DLS), ζ potential (ELS), specific surface area (BET), and metal/sulphur ratio (XRF) of $WS_2$ and $MoS_2$ ENMs

ENMs through the alveolar epithelial cell barrier unlikely and reasonably assimilates the biological impact of such ENMs to larger particles with size in the sub-micrometric range.

Since the surface charge of a particle is one of the key physico-chemical features relevant to understand the interaction between particles and the living matter, the ζ-potential of the dust samples suspended in cell growth culture medium (DMEM, buffered at pH 7.4) was measured. Under these conditions, ζ-potential of $WS_2$ and $MoS_2$ were −11 and −10 mV respectively. In vitro and in vivo studies demonstrated that negatively charged particles are generally less cytotoxic, less inflammogenic, and induce haemolysis and platelet aggregation to a lower extent than neutral or positive particles (Nel et al. 2009 and ref. therein). The negative net charge of $WS_2$ and $MoS_2$ surface may support a less hazardous interaction between ENMs and lung epithelial cells.

## Cytotoxicity

To evaluate the cytotoxic effect of $WS_2$ and $MoS_2$ ENMs, lactate dehydrogenase (LDH) released byA549 lung epithelial cells in the extracellular medium was measured (Polimeni et al. 2008). When cells are damaged, a release of LDH, a cytoplasmic enzyme, from the intracellular space into the extracellular medium occurs. This is one of the most sensitive methods to detect a perturbation of plasma membrane integrity, even when cells number and aspect are not yet modified. The release of LDH was detected by measuring the LDH activity through an enzymatic kinetic in the medium and in cell lysates.

In Fig. 3, the amount of LDH released into the extracellular space after 24 h of incubation with the $WS_2$ and $MoS_2$ ENMs is reported. Three different concentrations were investigated, namely 10, 25 and 50 μg of ENMs per $cm^2$ of cell culture. $WS_2$ was not able to induce a significant increase in LDH activity at any dose tested. $MoS_2$ did not exert any significant cytotoxic effect on A549 cells at low and intermediate doses (10 and 25 μg/$cm^2$ of cell culture, respectively), inducing significant increase in the extracellular LDH activity only at high dose (50 μg/$cm^2$ of cell culture).

## NO production

Nitric oxide (NO) is a highly reactive radical molecule involved in several different cellular function, including proliferation, differentiation, and apoptosis (Murphy 1999). The specific enzyme responsible for NO biosynthesis is the nitric oxide synthase (NOS) and converts L-arginine in L-citrulline and NO in cells with a 1:1 stoichiometry (Marletta 1993). According to the tissue distribution, NOS exists in different isoforms, and the inducible form (iNOS) can be expressed in response to different stimuli, including oxidative stress and inflammatory cytokines. Under oxidative stress conditions, NO is supposed to react with reactive oxygen species (ROS) causing an increased production of reactive nitrogen species (RNS) that potentiate cellular damage (Jorens et al. 1995; Laroux et al. 2001; Hsieh et al. 2014). The NO production may be assessed by measuring the extracellular levels of its stable derivative nitrite. After a 24 h incubation with ENMs, the extracellular levels of nitrite were measured in the supernatant of A549 cell cultures. Both $WS_2$ and $MoS_2$ did not stimulate nitrite production at any concentration tested (Fig. 4).

## GSH consumption

Glutathione is one of the most important antioxidant molecules in the cell. It is a cytoplasmic glycine–cysteine–glutamic acid tripeptide. The –SH group of its cysteine is highly sensitive to oxidation (Ghezzi 2011). Following an oxidative stress, glutathione (GSH) is oxidized to GSH disulphide (GSSG) to balance the excess of oxidizing species. GSSG is then

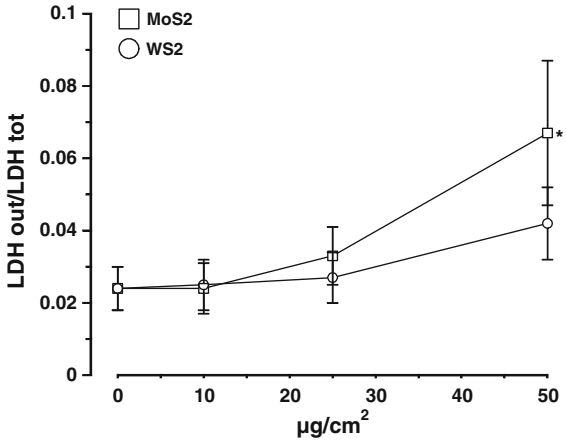


**Fig. 3** Relative release of lactate dehydrogenase (LDH) in the supernatant of A549 cells. Cells were incubated in the absence (0 µg/cm$^2$, ctrl) or presence of ENMs at the concentrations of 10, 25 and 50 µg/cm$^2$. After 24 h, the extracellular LDH activity was normalized by the total (intracellular + extracellular) LDH activity of the dish. Measurements were performed in duplicate, and data are presented as mean ± SEM ($n = 7$). Vs ctrl: $^*p < 0.04$

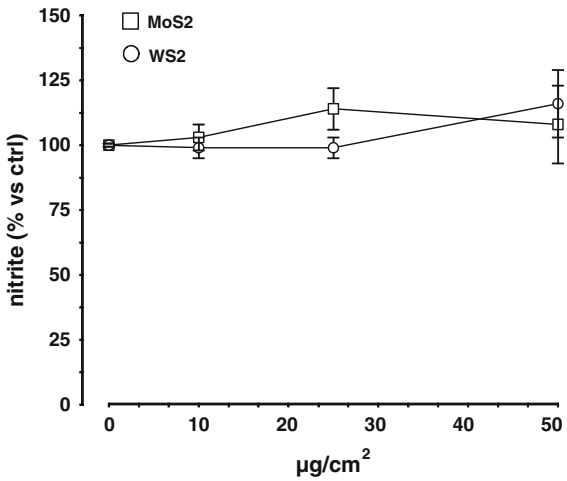


**Fig. 4** Extracellular levels of nitrite in A549 cells. Cells were incubated for 24 h in the absence (0 µg/cm$^2$, ctrl) or presence of ENMs at the concentrations of 10, 25 and 50 µg/cm$^2$. After the incubation, the nitrite accumulation in the culture supernatant was assessed. Measurements were performed in duplicate, and data are presented as mean ± SEM ($n = 7$)

reduced by the glutathione reductase to GSH. To evaluate if cells underwent an oxidative stress condition, the levels of intracellular GSH and GSSG were detected. After a 24 h incubation, $WS_2$ did not exert a significant decrease of the levels of GSH at any

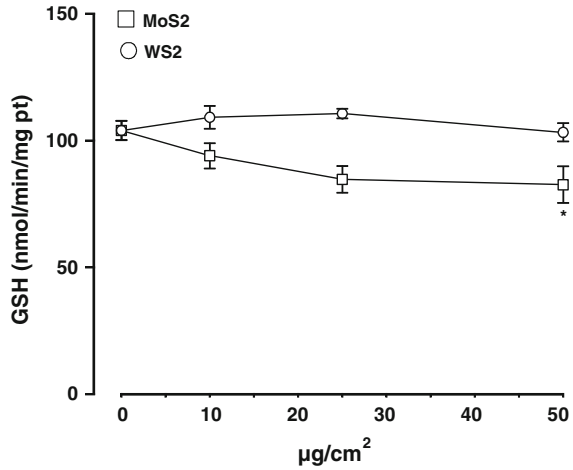


**Fig. 5** Intracellular levels of reduced glutathione in A549 cells. Cells were incubated for 24 h in the absence (0 µg/cm$^2$, ctrl) or presence of ENMs at the concentrations of 10, 25 and 50 µg/cm$^2$. Measurements were performed in duplicate, and data are presented as mean ± SEM ($n = 4$). Vs ctrl: $^*p < 0.04$

concentration tested. In the same conditions, only at the highest dose (50 µg/cm$^2$) $MoS_2$ showed a significant decrease in the GSH levels, while lower concentration of ENM did not modified the level of GSH by respect to the control (Fig. 5).

The cellular endpoints evaluated have a well-accepted validity in predicting the potential toxic effect of an inhaled ENM. They have been associated to several detrimental effects elicited by fibres, particles and nanoparticles (Gazzano et al. 2007; Ghiazza et al. 2011; Unfried et al. 2007). In particular, the general absence of a positive response in the three complementary tests carried out can reasonably be associated to a low toxic effect in the A549 human pulmonary cell line. The results of cellular tests are also in agreement with previous in vivo inhalation tests on a similar $WS_2$-based ENM, where no toxic reaction in short-term exposure was reported (Ganzlebe et al. 2011 and references therein).

## In vitro lipid peroxidation

Lipid peroxidation is a complex process in which unsaturated fatty acids undergo oxidation, via a free radical chain reaction, to a plurality of products. Lipid peroxidation is claimed to be the major contributor to cells membrane damage and implied in a several diseases (Dix and Aikens 1993).

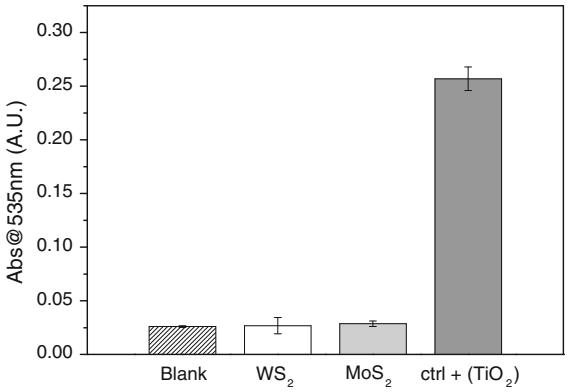


**Fig. 6** MDA–TBA complex absorbance (535 nm) recorded on the supernatant of $WS_2$ and $MoS_2$ suspensions in a buffered dispersion of linoleic acid. A suspension of linoleic acid without the dust and in the presence of nanometric $TiO_2$ was employed as negative (*blank*) and positive control (ctrl+), respectively

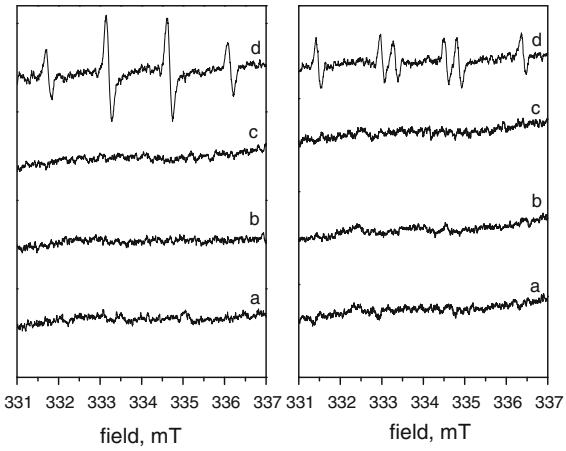


**Fig. 7** EPR spectra recorded on the supernatant of $WS_2$ (*b*) and $MoS_2$ (*c*) suspensions in a DMPO buffered solution after 60 min of incubation in the presence of $H_2O_2$ (*left panel*) and formate ion (*right panel*). The EPR spectra were recorded also in the absence of dust (blank solution, *a*) and in the presence of indium/tin oxide (positive control, *d*)

Reactive oxygen species (ROS) are implied in the reactivity of a variety of particulates toward lipids (Lison et al. 1995). Moreover several transition metals such as iron, copper and lead may act as initiators of the radical chain reaction responsible for lipid peroxidation via a mechanism possibly independent from ROS production, but not clearly understood (Halliwell and Chirico 1993). In the present work, the capability of $WS_2$ and $MoS_2$ to cause lipoperoxidation was investigated employing linoleic acid as target molecule, and measuring spectrophotometrically the amount of the end product malondialdehyde (MDA) via TBA assay. The autoxidative processes that may take place in the presence of $O_2$ were evaluated by performing the same experiment on a buffered dispersion of linoleic acid in the absence of the dust (referred to as *blank*). Figure 6 shows that the amount of MDA produced with $WS_2$ or $MoS_2$ and compares the ENMs response with a positive control obtained incubating nanometric $TiO_2$ with linoleic acid in the same experimental conditions. Both ENMs investigated oxidized linoleic acid to the same extent than the non-specific autoxidative process observed for linoleic acid alone (blank) and to a significantly lower extent that nano-$TiO_2$. This result indicates that both samples are not active in oxidizing linoleic acid in a cell-free environment. The comparison with lipoperoxidation induced by nano-$TiO_2$ (Turci et al. 2013), a safe and commonly used ENM, further highlights the low oxidative potential of $WS_2$ and $MoS_2$.

## Free radical release

Particles induced reactive oxygen species (ROS) and free radicals in general are involved in many detrimental effects on human health, inducing both direct and indirect macromolecules damage, nucleic acids oxidation, inflammation and cytotoxic effect (Fenoglio et al. 2011; Fubini et al. 2011). The release of radical species was monitored by electron paramagnetic resonance (EPR) by using the spin-trapping technique with DMPO.

Two radical-generating mechanisms were investigated:

(a) $HO^{\bullet}$ radical generation in the presence of hydrogen peroxide (the Fenton activity). This test mimics the contact with lysosomal fluids where $H_2O_2$ is released following phagocytosis by alveolar macrophages;
(b) $^{\bullet}COO^{-}$ from the formate ion used as a model target molecule for homolytic cleavage of a carbon–hydrogen bond of organic molecules.

The production of free radicals following the two abovementioned reactions was monitored with time recording EPR spectra on the dust suspension after 10, 30 and 60 min of incubation. Figure 7 reports the EPR spectra recorded after 60 min of incubation of the ENMs in the presence of $H_2O_2$ (left panel) and formate

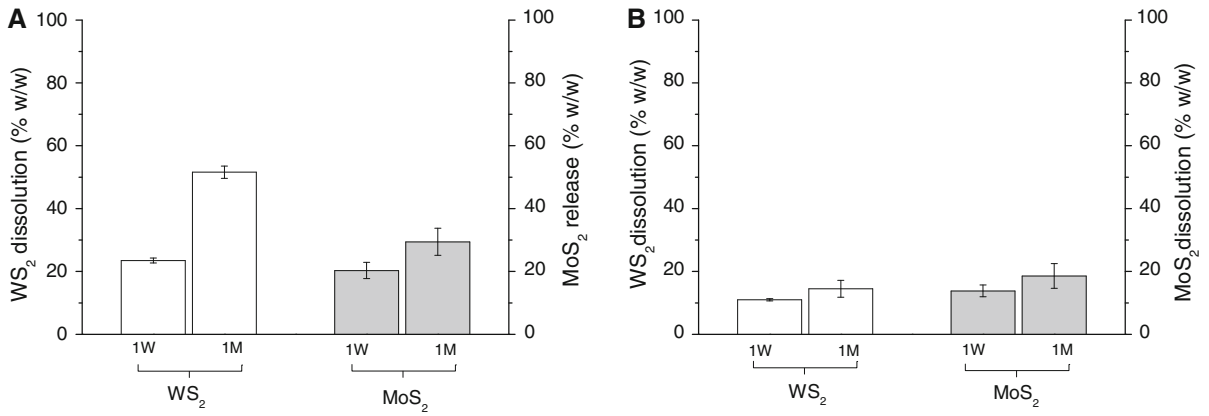


**Fig. 8** Amount of $WS_2$ (*white bars*) and $MoS_2$ (*grey bars*) dissolved in Gamble's solution (**a**) and in PSF (**b**) after one week (1 W *bars*) and one month (1 M *bars*) of incubation reported as wt%

ion (right panel), since identical spectra were recorded at shorter time points. The results obtained evidenced that, in the presence of $H_2O_2$, $HO^{\bullet}$ radical was not detected, thus indicating that the ENMs studied are not able to promote the release of ROS via Fenton-like reactivity. Moreover, in the presence of formate ion, no $^{\bullet}COO^{-}$ radical was detected with the ENMs studied. Such result indicates that dusts are not able to abstract hydrogen from C–H bond of organic molecules and are not likely to interfere via redox-reactions with biological molecules, including lipids, proteins and nucleic acids.

The comparison of the free-radical reactivity with indium/tin oxide, a well-assessed inflammatory and genotoxic industrial dust (Lison et al. 2009), tested in the same experimental conditions, gives further evidence of the generally negligible oxidative potential of $WS_2$ and $MoS_2$.

## Ion release in simulated biological fluids

Following exposure, inhaled particles come in contact with several extracellular and intracellular fluids and dissolution process strongly determine the fate of the particle inside the lung. For instance, the well-accepted paradigm for many toxic particulates, e.g. asbestos, includes the extraordinary long residence time of the fibre within the lung among the key factors in carcinogenesis (Donaldson et al. 2010). The ion release in a solution gives indirect information about the solubility related to the biopersistence of a particulate. Since the major route of exposure to the ENMs studied is the pulmonary one, we measured the ion release in two simulated biological fluids which mimic the bronchoalveolar fluid without proteins at physiological pH, and the vesicles involved in the processes of endo- and phagocytosis, the Gamble's solution (GS) and the phagolysosomal simulant fluid (PSF), respectively.

The relative amount of $WS_2$ and $MoS_2$ dissolved after one week (1 W) and one month (1 M) of incubation in GS and in PSF, expressed as wt% and measured with ICP–AES, is reported in Fig. 8a, b, respectively. Both samples are rather soluble in GS and PSF. After one week of incubation in GS, the dust dissolved was similar for both $WS_2$ and $MoS_2$ (ca. 20 %). This value increased for both the samples reaching ca. 50 % for $WS_2$ and ca. 30 % for $MoS_2$. In PSF, $WS_2$, and $MoS_2$ exhibited similar solubility (11 % for $WS_2$ and 14 % for $MoS_2$ after 1 week; 14 % for $WS_2$ and 19 % for $MoS_2$ after 1 month of incubation). The relevant solubility in simulated media suggests that both the neutral pulmonary extracellular fluid and the acidic environment of phagolysosomes actively concur to the clearance of ENMs eventually internalized into the lung.

## Conclusion

A toxicity screening that integrates in vitro cellular and a cell-free chemical approach was used and several aspects commonly associated to the toxic responses elicited by ENMs were evaluated. In all

tests, $WS_2$ did not elicit a response significantly different from the negative control, even at the highest dose tested. Similarly, a negligible cellular and chemical activity was shown by $MoS_2$, even if a moderate cellular toxicity was observed at the highest dose tested. A reasonably short residence time of the two ENMs in the lung was suggested by solubility tests. The in vitro toxicological screening carried out indicates that the overall biological and chemical reactivities of $WS_2$ and $MoS_2$ are low, and their potential hazard for human respiratory system could be rated from moderate to negligible in the context of an ERA and LCA.

**Acknowledgments** The ADDNANO project (no. 229284), funded by the European Commission as part of the 7th Framework Programme, is gratefully acknowledged for the financial support. The authors are particularly grateful to Prof. Fabrice Dassenoy (Ecole Centrale de Lyon, Ecully, France) for TEM analysis.

## References

Bensaid S, Deorsola FA, Marchisio DL, Russo N, Fino D (2014) Flow field simulation and mixing efficiency assessment of the multi-inlet vortex mixer for molybdenum sulfide nanoparticle precipitation. Chem Eng J 238:66–77. doi:10.1016/j.cej.2013.09.065

Bouwmeester H, Lynch I, Marvin HJP, Dawson KA, Berges M, Braguer D, Byrne HJ, Casey A, Chambers G, Clift MJD, Elia G, Fernandes TF, Fjellsbo LB, Hatto P, Juillerat L, Klein C, Kreyling WG, Nickel C, Riediker M, Stone V (2011) Minimal analytical characterization of engineered nanomaterials needed for hazard assessment in biological matrices. Nanotoxicology 5(1):1–11. doi:10.3109/17435391003775266

Cohen Y, Rallo R, Liu R, Liu HH (2013) In silico analysis of nanomaterials hazard and risk. Acc Chem Res 46(3):802–812. doi:10.1021/Ar300049e

Deorsola FA, Russo N, Blengini GA, Fino D (2012) Synthesis, characterization and environmental assessment of nano-sized $MoS_2$ particles for lubricants applications. Chem Eng J 195:1–6. doi:10.1016/j.cej.2012.04.080

Dix TA, Aikens J (1993) Mechanisms and biological relevance of lipid-peroxidation initiation. Chem Res Toxicol 6(1):2–18. doi:10.1021/Tx00031a001

Donaldson K, Murphy FA, Duffin R, Poland CA (2010) Asbestos, carbon nanotubes and the pleural mesothelium: a review of the hypothesis regarding the role of long fibre retention in the parietal pleura, inflammation and mesothelioma. Particle Fibre Toxicol 7. doi:10.1186/1743-8977-7-5

Donaldson K, Murphy F, Schinwald A, Duffin R, Poland CA (2011) Identifying the pulmonary hazard of high aspect ratio nanoparticles to enable their safety-by-design. Nanomedicine 6(1):143–156. doi:10.2217/nnm.10.139

Feldman Y, Frey GL, Homyonfer M, Lyakhovitskaya V, Margulis L, Cohen H, Hodes G, Hutchison JL, Tenne R (1996) Bulk synthesis of inorganic fullerene-like MS(2) (M = Mo, W) from the respective trioxides and the reaction mechanism. J Am Chem Soc 118(23):5362–5367. doi:10.1021/Ja9602408

Fenoglio I, Fubini B, Ghibaudi EM, Turci F (2011) Multiple aspects of the interaction of biomacromolecules with inorganic surfaces. Adv Drug Deliv Rev 63(13):1186–1209. doi:10.1016/j.addr.2011.08.001

Fino D, Deorsola F, Bensaid S, Russo N (2011) Nano-sized additive synthesis for lubricant oils and compatibility tests with after-treatment catalysts. SAE Technical Papers. doi:10.4271/2011-24-0101

Fubini B, Ghiazza M, Fenoglio I (2010) Physico-chemical features of engineered nanoparticles relevant to their toxicity. Nanotoxicology 4(4):347–363. doi:10.3109/17435390.2010.509519

Fubini B, Fenoglio I, Tomatis M, Turci F (2011) Effect of chemical composition and state of the surface on the toxic response to high aspect ratio nanomaterials. Nanomedicine 6(5):899–920. doi:10.2217/Nnm.11.80

Ganzlebe C, Pelsy F, Hansen SF, Corden C, Grebot B, Sobey M (2011) Review of environmental legislation for the regulatory control of nanomaterials—final report

Gazzano E, Turci F, Foresti E, Putzu MG, Aldieri E, Silvagno F, Lesci IG, Tomatis M, Riganti C, Romano C, Fubini B, Roveri N, Ghigo D (2007) Iron-loaded synthetic chrysotile: a new model solid for studying the role of iron in asbestos toxicity. Chem Res Toxicol 20(3):380–387. doi:10.1021/Tx600354f

Ghezzi P (2011) Role of glutathione in immunity and inflammation in the lung. Int J Gen Med 4:105–113. doi:10.2147/IJGM.S15618

Ghiazza M, Scherbart AM, Fenoglio I, Grendene F, Turci F, Martra G, Albrecht C, Schins RPF, Fubini B (2011) Surface iron inhibits quartz-induced cytotoxic and inflammatory responses in alveolar macrophages. Chem Res Toxicol 24(1):99–110. doi:10.1021/Tx1003003

Ghigo D, Aldieri E, Todde R, Costamagna C, Garbarino G, Pescarmona G, Bosia A (1998) Chloroquine stimulates nitric oxide synthesis in murine, porcine and human endothelial cells. J Clin Invest 3(102):595–605. doi:10.1172/JCI1052

Groppo C, Tomatis M, Turci F, Gazzano E, Ghigo D, Compagnoni R, Fubini B (2005) Potential toxicity of nonregulated asbestiform minerals: balangeroite from the western Alps. Part 1: identification and characterization. J Toxicol Environ Health A 68(1):1–19. doi:10.1080/15287390590523867

Halliwell B, Chirico S (1993) Lipid-peroxidation: its mechanism, measurement, and significance. Am J Clin Nutr 57(5):S715–S725

Hsieh HJ, Liu CA, Huang B, Tseng AHH, Wang DL (2014) Shear-induced endothelial mechanotransduction: the interplay between reactive oxygen species (ROS) and nitric oxide (NO) and the pathophysiological implications. J Biomed Sci 21. doi: 10.1186/1423-0127-21-3

Jorens PG, Matthys KE, Bult H (1995) Modulation of nitric-oxide synthase activity in macrophages. Mediators Inflamm 4(2):75–89. doi:10.1155/S0962935195000135

Laroux FS, Pavlick KP, Hines IN, Kawachi S, Harada H, Bharwani S, Hoffman JM, Grisham MB (2001) Role of nitric oxide in inflammation. Acta Physiol Scand 173(1):113–118. doi:10.1046/j.1365-201X.2001.00891.x

Lison D, Carbonnelle P, Mollo L, Lauwerys R, Fubini B (1995) Physicochemical mechanism of the interaction between cobalt metal and carbide particles to generate toxic activated oxygen species. Chem Res Toxicol 8(4):600–606. doi:10.1021/Tx00046a015

Lison D, Laloy J, Corazzari I, Muller J, Rabolli V, Panin N, Huaux F, Fenoglio I, Fubini B (2009) Sintered indium-tin-oxide (ITO) particles: a new pneumotoxic entity. Toxicol Sci 108(2):472–481. doi:10.1093/toxsci/kfp014

Margulis L, Salitra G, Tenne R, Talianker M (1993) Nested fullerene-like structures. Nature 365(6442):113–114. doi:10.1038/365113b0

Marletta MA (1993) Nitric-oxide synthase structure and mechanism. J Biol Chem 268(17):12231–12234

Marques MRC, Loebenberg R, Almukainzi M (2011) Simulated biological fluids with possible application in dissolution testing. Dissolut Technol 18(3):15–28

Murphy MP (1999) Nitric oxide and cell death. Biochimica Et Biophysica Acta-Bioenergetics 1411(2–3):401–414. doi:10.1016/S0005-2728(99)00029-8

Nel A, Xia T, Madler L, Li N (2006) Toxic potential of materials at the nanolevel. Science 311(5761):622–627. doi:10.1126/science.1114397

Nel AE, Madler L, Velegol D, Xia T, Hoek EMV, Somasundaran P, Klaessig F, Castranova V, Thompson M (2009) Understanding biophysicochemical interactions at the nano-bio interface. Nat Mater 8(7):543–557. doi:10.1038/Nmat2442

Nel A, Xia T, Meng H, Wang X, Lin SJ, Ji ZX, Zhang HY (2013) Nanomaterial toxicity testing in the 21st century: use of a predictive toxicological approach and high-throughput screening. Acc Chem Res 46(3):607–621. doi:10.1021/Ar300022h

Oberdorster G (2010) Safety assessment for nanotechnology and nanomedicine: concepts of nanotoxicology. J Intern Med 267(1):89–105. doi:10.1111/j.1365-2796.2009.02187.x

Oberdorster G, Sharp Z, Atudorei V, Elder A, Gelein R, Kreyling W, Cox C (2004) Translocation of inhaled ultrafine particles to the brain. Inhal Toxicol 16(6–7):437–445. doi:10.1080/08958370490439597

Oberdorster G, Oberdorster E, Oberdorster J (2005) Nanotoxicology: an emerging discipline evolving from studies of ultrafine particles. Environ Health Perspect 113(7):823–839. doi:10.1289/Ehp.7339

Podila R, Brown JM (2013) Toxicity of engineered nanomaterials: a physicochemical perspective. J Biochem Mol Toxicol 27(1):50–55. doi:10.1002/Jbt.21442

Polimeni M, Gazzano E, Ghiazza M, Fenoglio I, Bosia A, Fubini B, Ghigo D (2008) Quartz inhibits glucose 6-phosphate dehydrogenase in murine alveolar macrophages. Chem Res Toxicol 21(4):888–894. doi:10.1021/Tx7003213

Raimondi A, Girotti G, Blengini GA, Fino D (2012) LCA of petroleum-based lubricants: state of art and inclusion of additives. Int J Life Cycle Assess 17(8):987–996. doi:10.1007/s11367-012-0437-4

Santillo G, Deorsola FA, Bensaid S, Russo N, Fino D (2012) MoS2 nanoparticle precipitation in turbulent micromixers. Chem Eng J 207:322–328. doi:10.1016/j.cej.2012.06.127

Som C, Nowack B, Krug HF, Wick P (2013) Toward the development of decision supporting tools that can be used for safe production and use of nanomaterials. Acc Chem Res 46(3):863–872. doi:10.1021/Ar3000458

Spikes H (2004) The history and mechanisms of ZDDP. Tribol Lett 17(3):469–489. doi:10.1023/B:Tril.0000044495.26882.B5

Stefaniak AB, Guilmette RA, Day GA, Hoover MD, Breysse PN, Scripsick RC (2005) Characterization of phagolysosomal simulant fluid for study of beryllium aerosol particle dissolution. Toxicol In Vitro 19(1):123–134. doi:10.1016/j.tiv.2004.08.001

Stern ST, McNeil SE (2008) Nanotechnology safety concerns revisited. Toxicol Sci 101(1):4–21. doi:10.1093/toxsci/kfm169

Tenne R, Margulis L, Genut M, Hodes G (1992) Polyhedral and cylindrical structures of tungsten disulfide. Nature 360(6403):444–446. doi:10.1038/360444a0

Turci F, Colonna M, Tomatis M, Mantegna S, Cravotto G, Gulino G, Aldieri E, Ghigo D, Fubini B (2012) Surface reactivity and cell responses to chrysotile asbestos nanofibers. Chem Res Toxicol 25(4):884–894. doi:10.1021/Tx2005019

Turci F, Peira E, Corazzari I, Fenoglio I, Trotta M, Fubini B (2013) Crystalline phase modulates the potency of nanometric $TiO_2$ to adhere to and perturb the stratum corneum of porcine skin under indoor light. Chem Res Toxicol 26(10):1579–1590. doi:10.1021/Tx400285j

Unfried K, Albrecht C, Klotz LO, Von Mikecz A, Grether-Beck S, Schins RPF (2007) Cellular responses to nanoparticles: target structures and mechanisms. Nanotoxicology 1(1):52–71. doi:10.1080/00222930701314932

Vandeputte C, Guizon I, Genestie-denis I, Vannier B, Lorenzon G (1994) A microtiter assay for total glutathione and glutathione disulfide contents in cultured/isolated cells: performance study of a new miniaturized protocol. Cell Biol Toxicol 10:415–421

Wang JF, Gerlach JD, Savage N, Cobb GP (2013) Necessity and approach to integrated nanomaterial legislation and governance. Sci Total Environ 442:56–62. doi:10.1016/j.scitotenv.2012.09.073

Xia T, Malasarn D, Lin SJ, Ji ZX, Zhang HY, Miller RJ, Keller AA, Nisbet RM, Harthorn BH, Godwin HA, Lenihan HS, Liu R, Gardea-Torresdey J, Cohen Y, Madler L, Holden PA, Zink JI, Nel AE (2013) Implementation of a multidisciplinary approach to solve complex nano EHS problems by the UC center for the environmental implications of nanotechnology. Small 9(9–10):1428–1443. doi:10.1002/smll.201201700

Zhang HY, Ji ZX, Xia T, Meng H, Low-Kam C, Liu R, Pokhrel S, Lin SJ, Wang X, Liao YP, Wang MY, Li LJ, Rallo R, Damoiseaux R, Telesca D, Madler L, Cohen Y, Zink JI, Nel AE (2012) Use of metal oxide nanoparticle band gap to develop a predictive paradigm for oxidative stress and acute pulmonary inflammation. ACS Nano 6(5):4349–4368. doi:10.1021/Nn3010087